# Metal-Mediated Reaction Modeled on Nature: The Activation of Isothiocyanates Initiated by Zinc Thiolate Complexes

Wilhelm A. Eger,[†,‡] Martin Presselt,[§,⊥] Burkhard O. Jahn,[†,¶] Michael Schmitt,[§] Jürgen Popp,[§] and Ernst Anders[*,†]

[†]Institut für Organische Chemie und Makromolekulare Chemie, Friedrich-Schiller-Universität Jena, Humboldtstrasse 10, 07743 Jena, Germany

[§]Institut für Physikalische Chemie, Friedrich-Schiller-Universität Jena, Helmholzweg 4, 07743 Jena, Germany

[‡]School of Molecular Chemistry and Bioscience, University of Queensland, Building 68, St. Lucia, Brisbane, 4072 Queensland, Australia

[⊥]Institute of Physics, Ilmenau University of Technology, Weimarer Strasse 32, 98693 Ilmenau, Germany

[¶]Institute of Organic Chemistry and Biochemistry AV CR, Flemingovo namesti 2, Prague 16610, Czech Republic

Ⓢ Supporting Information

ABSTRACT: On the basis of detailed theoretical studies of the mode of action of carbonic anhydrase (CA) and models resembling only its reactive core, a complete computational pathway analysis of the reaction between several isothiocyanates and methyl mercaptan activated by a thiolate-bearing model complex $[Zn(NH_3)_3SMe]^+$ was performed at a high level of density functional theory (DFT). Furthermore, model reactions have been studied in the experiment using relatively stable zinc complexes and have been investigated by gas chromatography/mass spectrometry and Raman spectroscopy. The model complexes used in the experiment are based upon the well-known azamacrocyclic ligand family ([12]aneN_4, [14]aneN_4, i-[14]aneN_4, and [15]aneN_4) and are commonly formulated as ([Zn-([X]aneN_4)(SBn)]ClO_4. As predicted by our DFT calculations, all of these complexes are capable of insertion into the heterocumulene system. Raman spectroscopic investigations indicate that aryl-substituted isothiocyanates predominantly add to the C=N bond and that the size of the ring-shaped ligands of the zinc complex also has a very significant influence on the selectivity and on the reactivity as well. Unfortunately, the activated isothiocyanate is not able to add to the thiolate-corresponding mercaptan to invoke a CA analogous catalytic cycle. However, more reactive compounds such as methyl iodide can be incorporated. This work gives new insight into the mode of action and reaction path variants derived from the CA principles. Further, aspects of the reliability of DFT calculations concerning the prediction of the selectivity and reactivity are discussed. In addition, the presented synthetic pathways can offer a completely new access to a variety of dithiocarbamates.
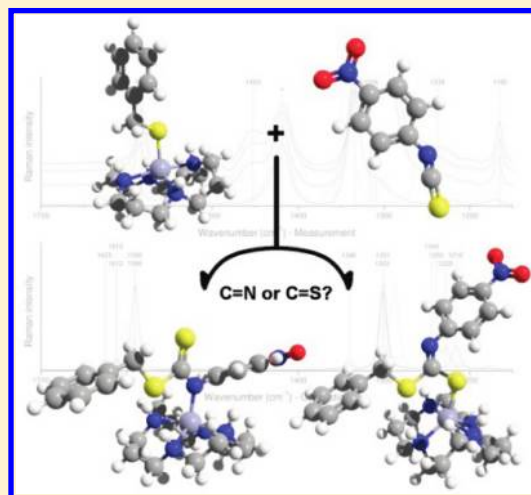
INTRODUCTION

The class of carbonic anhydrases (CAs) includes one of the fastest known enzymes. The CAs catalyze the reaction of water and cumulene carbon dioxide (CO_2) to give bicarbonate and a proton.[1] They are remarkably efficient at accelerating this reaction and possess molecular activities up to 10^6 s^{-1}.[2]

CAs are located both in red blood cells to facilitate CO_2 transport[3] and in tissues like the gall bladder epithelium or secretory epithelia in kidneys to accelerate electrolyte secretion.[4] CAs belong to the zinc metalloenzymes and possess a Zn^{2+} cation,[5] which is essential for catalysis. The metal cation is surrounded by three histidine ligands and one hydroxide ion in an almost ideal tetrahedral coordination sphere.

For its speed and ability to activate a more or less inert molecule such as CO_2, the paragon CA is a suitable candidate for biomimetic catalysis.[6]

In the past, several attempts were made to explain the mode of action of CA. Most of them used quantum mechanical, in particular density functional theory (DFT), calculations to estimate the activation barriers and to provide insight into the reaction pathways.[7] In parallel, bioanalogue catalytic cycles, in which a variety of (hetero)cumulenic molecules such as carbonyl sulfide,[8] allenes,[9] and isothiocyanates replace CO_2, have also been investigated.[10] The aim of these calculations was to transcribe the reaction principle of CA to *synthetic chemistry* using a catalytically active model complex. In a preceding investigation, we showed that the bioanalogue reaction of CS_2 and CA modeling zinc thiolate complexes is considered to be working.[11] Thus, it is of interest to check whether a CA-derived

Scheme 1. Common Reaction Scheme of the Reaction of Isothiocyanates with Zinc Thiolate Complexes
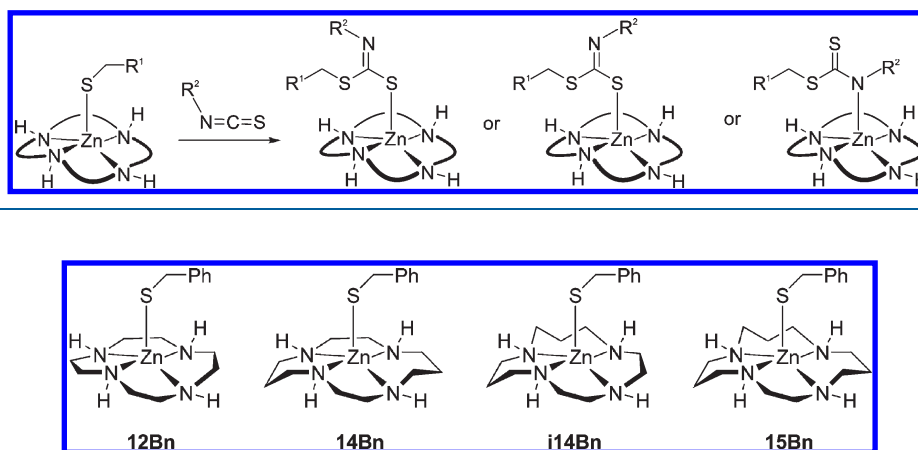

Figure 1. Benzylzinc thiolate complexes used in this work.

model complex is able to fixate and activate isothiocyanates analogously to the mode of action given by nature.

In the present paper, we will discuss both the experimental realization based upon Raman spectroscopy and gas chromatography/mass spectrometry (GC/MS) measurements and the theoretical interpretation using high-level DFT calculations to investigate the reaction mode of isothiocyanates with zinc thiolate complexes and of the subsequent transformations (cf. Scheme 1) with methyl mercaptan. Dithiocarbamates, possible products of this reaction, are of general increasing interest because they can be used, for example, as improved linkers to gold surfaces, thus being an appealing alternative to the common thiols.[12] Furthermore, dithiocarbamate derivatives are widely used as pesticides and, in particular, as fungicides.[13]

■ RESULTS AND DISCUSSION

Models. Most of our preceding theoretical studies about CA analogues and their mechanisms of cumulene activations and transformations have been performed using a simplified model structure of the active site, the $[Zn(NH_3)_3OH]^+$ complex. Because this species only exists in the gas phase under specific conditions,[14] it is not appropriate to use it for experimental purposes. Nevertheless, because the most important structural and electronic properties agree well with those of much larger structures, it therefore allows reliable DFT-based predictions. Especially, the structural agreement with complexes built from well-established ligands (e.g., specific azamacrocycles), which are commonly used for the construction of such CA-simulating zinc model complexes and for the investigation of the mode of action of the enzyme, is very good.[15] Because most of these complexes contain a hydroxyl group to incorporate the *natural* nucleophilic ligand, we recently developed catalyst models that include (nucleophilic) thiolate groups and that were investigated concerning their behavior against cumulenes, e.g., CS_2.[11,16] For several reasons (especially with respect to a future application in syntheses), some advantages appear to be promising for the use of these thiolate complexes. First, they are soluble in aprotic solvents, a very important aspect. Second, they do not collapse to give di- or trimers like the hydroxyl complexes[15a] and, therefore, do not shield their catalytic center. Third and finally, the missing

proton at the nucleophilic ligand will simplify the reaction mechanism (cf. the Zinc-Complex-Mediated Reactions section).

Because alkyl thiolate complexes are found to be unstable,[16] we chose the benzyl thiolate complexes of the following azamacrocycles: [12]aneN₄ ($[Zn([12]aneN_4)(SBn)]ClO_4$, **12Bn**), [14]aneN₄ ($[Zn([14]aneN_4)(SBn)]ClO_4$, **14Bn**), i-[14]aneN₄ ($[Zn(i-[14]aneN_4)-(SBn)]ClO_4$, **i14Bn**), and [15]aneN₄ ($[Zn([15]aneN_4)(SBn)]ClO_4$, **15Bn**) [numbers in brackets indicate the ring size, whereas the last letter and number mean the count of possible coordinating atoms; cf. Figure 1]. The reason for the choice of models with four nitrogen atoms complexing the zinc cation instead of three is the considerably better reactivity of these species.[17] For economic reasons, we calculated the pathway using the model $[Zn(NH_3)_3SMe]^+$. In the Computational Methods section, some technical details of the DFT and ab initio calculations are summarized.

Calculations. In a recent work, the geometries and energies of all important states within the postulated catalytic cycle of a CA model and isothiocyanate derivatives were extensively studied.[10] From these investigations, we concluded that it should be possible to activate the isothiocyanate group and to understand and finally profit from important steric and electronic properties. In particular, significant changes in the bond order, bond strength, and π-electron delocalization as well as changes within the force constant of a corresponding localized normal mode, polarizability, and electronic absorption are expected. While we used the $[Zn(NH_3)_3OH]^+$ model and water as the nucleophilic reagent in the preceding work, we now present the DFT calculations for the reaction of alkyl and aryl isothiocyanates with methyl mercaptan as a substitute for a HX compound, which should function as a reactant to allow construction of a catalytic cycle with $[Zn(NH_3)_3SR]^+$ as the model complex. To estimate the influence of different residues, all calculations were carried out with methyl, phenyl, and p-nitropenyl isothiocyanate.

Standard Reaction. Because isothiocyanates are only soluble in aprotic solvents, we did not consider water-catalyzed reaction paths.[10] When the free energies of the encounter complexes (**U-1**) and the three first transition states (**U-2(ts)**, **U-3(ts)**, and **U-4(ts)**) are compared with the enthalpies of the standard reaction of water with methyl isothiocyanate, a decrease in the energetic values can be observed (cf. Scheme 2, Table 1, the Supporting Information, and ref 10).

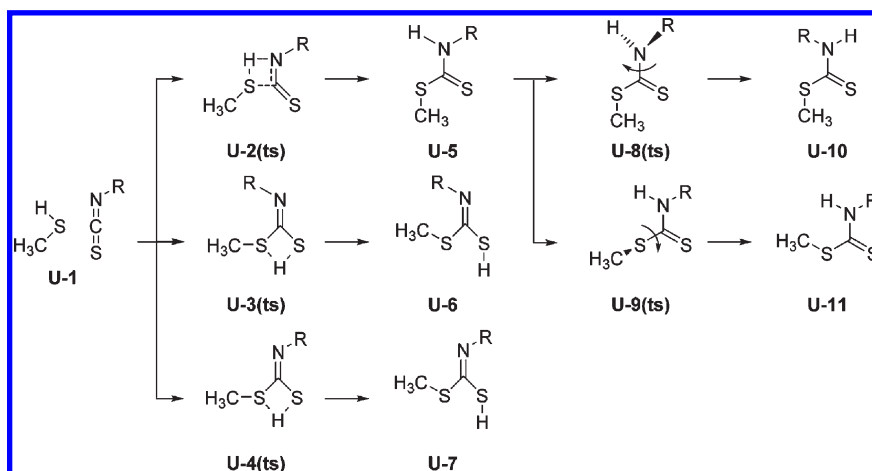**Scheme 2. Standard Reaction of Isothiocyanates with Methyl Mercaptan**

Table 1. Free Energies (kJ/mol) Corresponding to Scheme 2 with Different Isothiocyanates Relative to the Separated Reactants R-Isothiocyanate and Methyl Mercaptan at the MP2/aug-cc-pVDZ Level of Theory

	R = methyl		R = phenyl		R = p-NO₂-phenyl	
	ΔG	$\Delta\Delta G_a{}^a$	ΔG	$\Delta\Delta G_a$	ΔG	$\Delta\Delta G_a$
U-1	13		10		8	
U-2(ts)	159	146	151	141	148	140
U-3(ts)	166	153	163	153	155	147
U-4(ts)	167	154	161	151	155	147
U-5	−15		−2		−5	
U-6	55		37		32	
U-7	30		20		12	
U-8(ts)	49	64	44	46	37	42
U-9(ts)	15	30	27	29	25	30
U-10	−10		−8		−6	
U-11	0		13		11	

^{a} Activation energy relative to the preceding intermediate.

They result from a lower ring strain; as in the case of the reaction with water, the ring contains an oxygen and a sulfur atom instead of two sulfur atoms.[10] The slight decrease of the energetic values going from R = methyl to p-nitrophenyl is in good agreement with the stabilizing delocalization effects of the phenyl moieties. This is also due to the higher electron density of the C—N bond compared to the C—S bond, resulting from the electron-withdrawing effect increasing from R = methyl to p-nitrophenyl (cf. the Electronic Properties of Isothiocyanates section). Thus, the transition state U-2(ts) and the attack of the C—N bond are preferred throughout. The increase in the free energy of U-11 in the case of R = phenyl and p-nitrophenyl compared to methyl is due to hyperconjugation because the phenyl residues are able to generate a mesomeric system with the double bond.

The differences between U-10 and U-11 are the result of steric hindrance. In summary, this reaction is slightly exergonic relative to the separated reactants in the cases of U-5 and U-10 (cf. Scheme 2 and Table 1). Both intermediates are accessible via the transition state U-2(ts), which possesses the lowest activation

barrier of all insertion step possibilities, and therefore the C—N attack is preferred. Varying the residue of the isothiocyanate from R = methyl to p-nitrophenyl results in a more flattened hypersurface, in which the free energies of the transition states and intermediates, which are higher in enthalpy than the separated reactants, are lowered while those of the exergonic intermediates are increased. Solvent corrections using the geometries of the favored transition state U-2(ts) and the thermodynamically most stable products U-5 and U-10 show an increase of 30 kJ/mol in the case of the transition state and a decrease of 10 kJ/mol for the product. Thus, on the one hand, the reaction is thermodynamically favored, but, on the other hand, it is kinetically more hindered. Because the activation barriers of U-8(ts) and U-9(ts) are relatively low, U-10 and U-11 can exist at equilibrium. The solvent-corrected values can be found in the Supporting Information.

Zinc-Complex-Mediated Reactions. Analogously to the standard reaction, we calculated the zinc-complex-mediated versions of the reaction paths for several isothiocyanates. In comparison to the hydration reaction catalyzed by a $[Zn(NH_3)_3OH]^+$ model,[10] the reaction paths are simplified because the existence of the methyl group excludes complications resulting from proton shifts (equivalent to the Lipscomb mechanism; see ref 18). Therefore, only rotational transition states must be taken into account (equivalent to the Lindskog mechanism; see Scheme 3 and ref 19). Because two different transition states resembling the attack on the C—S bond (such as calculated before in the reaction cycle with water[10]) can only be found in the gas phase and with the substrate methyl isothiocyanate, this reaction path is not included in the scheme.

Both possibilities of attacking the cumulenic system result in only one intermediate each (5-A and N5-A; Scheme 3), both of which are able to transform via rotation of the C—S bond to either 5-B or N5-B (Scheme 4). Starting from these four intermediates, a mercaptan (or a HX compound) can add to each of them via either six- or four-membered cyclic transition states (e.g., Scheme 4). Thus, eight reaction pathways are conceivable (cf. the Supporting Information).

Regarding the free energies of these structures (cf. Tables 2 and 3), the influence of the solvent can be estimated. Whereas the attack on the C═S bond (2(ts)) is thoroughly preferred in the case of all isothiocyanates in the gas phase, the solvent-corrected

Scheme 3. Possible Addition Scenarios of Different Isothiocyanates
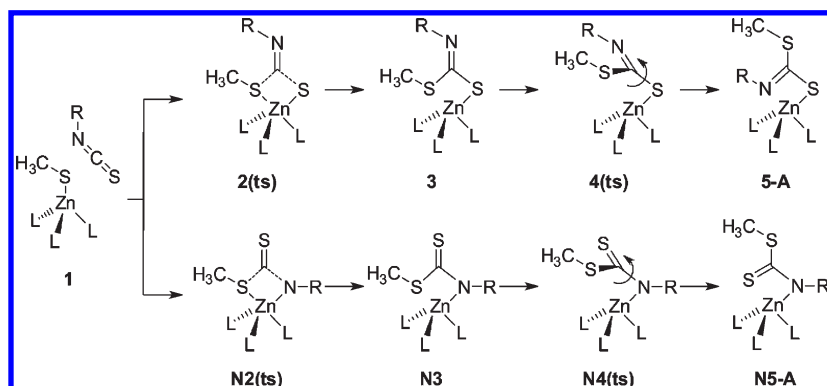
Scheme 4. Mechanistic Details of the Coordination Change after the Lindskog Rotation Transition State
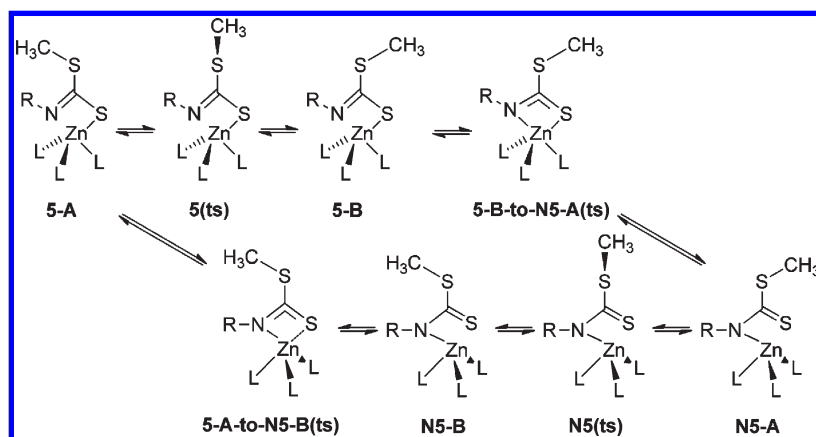
Table 2. Free Energies (kJ/mol) Corresponding to Scheme 3 and Several Isothiocyanates Relative to the Separated Reactants $[Zn(NH_3)_3SMe]^+$ and R-Isothiocyanate at the B3LYP/6-311+G(d,p) Level of Theory

	R = Me		R = Me*[a]		R = Ph		R = Ph*		R = p-NO$_2$-Ph		R = p-NO$_2$-Ph*	
	ΔG	$\Delta\Delta G_a$[b]	ΔG	$\Delta\Delta G_a$	ΔG	$\Delta\Delta G_a$	ΔG	$\Delta\Delta G_a$	ΔG	$\Delta\Delta G_a$	ΔG	$\Delta\Delta G_a$
1	6		40		6		43		25		41	
2(ts)	100	94	132	92	102	96	126	82	119	94	115	73
3	79		95		73		89		81		68	
4(ts)	90	11	100	5	86	13	90	1	93	12	76	8
5-A	52		83		44		76		56		59	
N2(ts)	127	121	128	88	125	119	126	83	142	117	112	70
N3	78		68		73		72		91		63	
N4(ts)	132	54	152	84	126	53	139	67	129	38	106	43
N5-A	24		65		23		66		37		55	

[a] Columns with stars represent solvent calculations in DMSO. [b] Activation energy relative to the preceding intermediate.

values do not differ significantly. The same behavior can be observed in all other cases except the rotation transition states **4(ts)** and **N4(ts)**. Contrary to the C—N bond, the rotation around the C—S bond in **4(ts)** is energetically lower because this bond is longer and the sulfur atom is much softer in terms of the hard and soft acids and bases principle. As a result, there are smaller steric and electronic hindrances in the case of **4(ts)**,

which makes this pathway slightly preferable. Both rotation bonds possess a significant amount of π molecular orbital and thus partial double-bond character. Nevertheless, the amount of this bonding character is nearly equal in both bonds and is therefore obviously not the reason for the energetic difference. Interestingly, the energies of nitrophenyl isothiocyanate are affected significantly more in comparison to the other

Table 3. Free Energies (kJ/mol) Corresponding to Scheme 4 and Several Isothiocyanates Relative to the Separated Reactants $[Zn(NH_3)_3SMe]^+$ and R-Isothiocyanate at the B3LYP/6-311+G(d,p) Level of Theory

	R = Me		R = Me*[a]		R = Ph		R = Ph*		R = p-NO$_2$-Ph		R = p-NO$_2$-Ph*	
	ΔG	$\Delta\Delta G_a{}^b$	ΔG	$\Delta\Delta G_a$	ΔG	$\Delta\Delta G_a$	ΔG	$\Delta\Delta G_a$	ΔG	$\Delta\Delta G_a$	ΔG	$\Delta\Delta G_a$
5-A	52		83		44		76		56		59	
5(ts)	58	6	86	3	62	18	85	9	74	18	74	15
5-B	28		67		28		64		39		38	
5-A-to−N5-B(ts)	63	11	94	11	54	10	95	19	72	16	89	30
N5-A	24		65		23		66		37		55	
N5(ts)	58	34	95	30	62	39	95	29	81	44	91	36
N5−B	63		85		28		87		62		78	
5-B-to-N5-A(ts)	30	2	74	7	29	1	76	12	45	6	73	35

^{a} Columns with stars represent solvent calculations in DMSO. ^{b} Activation energy relative to the preceding intermediate.

Scheme 5. Two Pathways Leading to the Most Stable Product, U-10
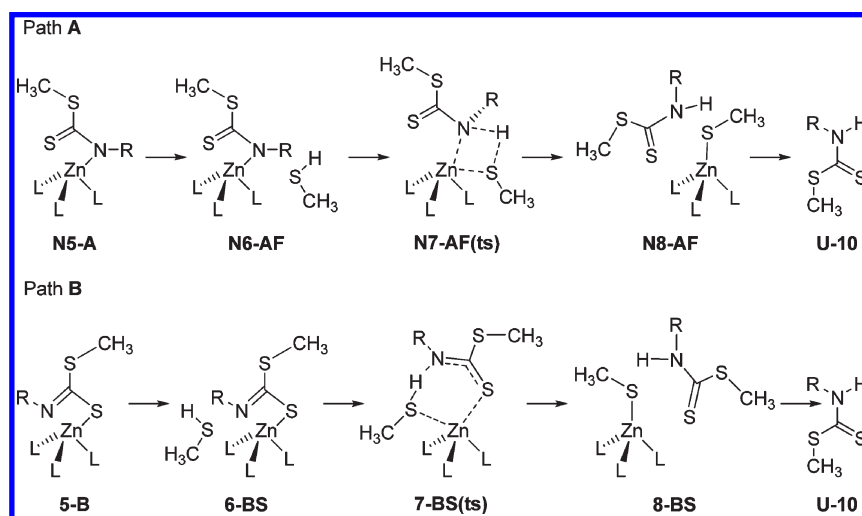
isothiocyanates. An explanation of this effect is the strong interaction of the nitro residue with the solvent field.

Following the intermediates **5-A** and **N5-A**, either the rotational transition states (**5(ts)** or **N5(ts)**) can be generated, which twist the outstanding methyl group around 180°, or a coordination change between the nitrogen and sulfur atoms (**A(ts)** or **B(ts)**) can take place. Because the activation barriers of these transition states are not very high, it is reasonable to assume that the pathways easily can change again at this point.

Accordingly, the selectivity at the rate-determining step does not define the selectivity of the product. Although the insertion into the C—S bond is energetically lowered, **N5-A** can be the overall preferred intermediate of the insertion step because it is in equilibrium with **5-A**.

Analogously to the pathway of CO_2 in CA and the reaction of isothiocyanate with water via a $[Zn(NH_3)_3OH]^+$ complex, the attack on comparable intermediates of the reaction with a $[Zn(NH_3)_3SMe]^+$ complex continues either via a four-membered cyclic (**F**) or a six-membered cyclic (**S**) transition state (cf. Scheme 5 and the Supporting Information). Looking at the products of all possible reaction paths, only one exergonic structure (**U-10**) can be found. This reduces the number of possible pathways to two (cf. Scheme 5). Path **A** proceeds via **N5-A** and reaches **U-10** via the four-membered cyclic transition state

N7-AF(ts) (cf. Scheme 5), while path **B** starts directly from **5-A** via **5(ts)** to **5-B** and continues via the six-membered transition state **7-BS(ts)** (cf. Schemes 4 and 5).

Not surprisingly, pathway **B** is preferred because the less strained transition state **7-BS(ts)** has significantly lower energies, which is most pronounced in the reaction of the aryl isothiocyanates.

Although the attack on the C═S double bond is favored in the gas phase, the calculations are not able to clear the selectivity problem because the energies of both transition states do not differ significantly, e.g., in dimethyl sulfoxide (DMSO). A possible selectivity in the first step would be almost lost after surmounting the rotation transition states because the following intermediates are all connected via very low transition states in the gas phase as well as in DMSO. In a comparison of the only two ways that lead to the thermodynamically most stable product, the route via the six-membered cyclic transition state appears to be the most favored one. Even though the energy of the last transition state is rather high and might be a problem.

Electronic Properties of Isothiocyanates. To examine the bonding situation in the cumulenic system, Natural Resonance Theory (NRT) calculations (as included in the *NBO* program package) were performed.[20] The NRT calculations resulted in 30% triple-bond character of the C—N bond in the case of

phenyl isothiocyanate and 0% in the case of methyl isothiocyanate. By inspection of the p-nitrophenyl isothiocyanate, we found 100% triple-bond character for the C—N bond. Because of the higher electron density in the C=N double bond, the addition to this bond is expected to be facilitated and thus favored over the C—S addition. Interestingly, this is not supported by calculation of the zinc-mediated pathway (cf. Schemes 3 and 4); in fact, they propose a slight preference of the C—S addition. In contrast, the calculations of the standard reaction path resemble the expected behavior very well. This is in agreement with the results of an extensive study concerning the influence of various substituents on phenyl, stating that a nitro group decreases the π character of the bond in the para position. Consequently, introduction of the nitro group leads to a less delocalized π-electron system.[21]

GC/MS. ^{1}H NMR investigations were performed (cf. Supporting Information), but unfortunately this appears not to be a sufficiently reliable tool for the decision on whether the C=N or C=S double bond was attacked.

To examine experimentally whether isothiocyanates insert or not, equimolar amounts of methyl, phenyl, and p-nitrophenyl isothiocyanate were each reacted with all complexes shown in Figure 1. After 10 min, they were quenched with methyl iodide to give zinc iodide complexes and methylated products (**A1**, **B1**, and **C1**; see Figure 2). In the case of p-nitrophenyl isothiocyanate, the solution immediately turns from yellow to red upon the insertion step and slowly back to yellow when methyl iodide is added. The existence of the mole peak of the products in the MS spectrum of the product peak in the GC spectra proves that methyl iodide reacted with one of the insertion intermediates, as depicted in Scheme 1, to give compound **A1**, **B1**, or **C1** (cf. Figure 2) and not directly with free isothiocyanate.

In addition to the zinc-complex-mediated insertion step, we examined the standard reaction between each isothiocyanate and

benzyl mercaptan under the same conditions and *observed no reaction at all*.

Furthermore, quenching the insertion intermediate with benzyl mercaptan was not successful at room temperature and higher temperatures. Although the red color of the solution turned to yellow again after the addition of a large excess of benzyl mercaptan at room temperature, no product could be found. Thus, a ligand exchange and subsequent decomposition of the inserted product back to the reactants must have occurred.

The problem could be not only the relatively high activation barrier of the last transition state **N7-BS(ts)** (cf. Table 4) but also the missing formation of the thermodynamically very stable Zn—I bond resulting from reaction with methyl iodide. Moreover, unfortunately, the applied method is not suitable to distinguish between the two isomers of the product because they do not separate well on the column and affords relatively high temperatures, which could initiate rearrangements. Thus, GC/MS is not the appropriate method for conclusions regarding the selectivity. Nevertheless, it is possible to give a rough description of the yields of the reactions because the peaks of the reactants, products, and decomposition products are all available.

The calculated yields are assembled in Table 5. As expected, the reaction with methyl isothiocyanate has the poorest yield because it is not activated as much as aryl isothiocyanates. However, there is also a correlation between the reactivity and structure of the zinc thiolate complexes used. While **15Bn** and **14Bn** have thoroughly good yields, **i14Bn** is not able to react with methyl isothiocyanate anymore and **12Bn** has very poor yield except in the case of the reaction with p-nitrophenyl isothiocyanate.

Raman Spectroscopy. To gain deeper insight into the reaction mechanism, Raman spectroscopy was applied. In particular, structural changes induced upon insertion into the electron-rich C=N or C=S bond of the isothiocyanate group are expected to give rise to significant changes in the Raman spectra. This assumption is justified by the fact that the vibrational transition energy, i.e., the wavenumber value of a normal mode involving the isothiocyanate group, is related to the bond strength as well as the bond order, while the corresponding Raman intensity is related to the electron delocalization.[22] Consequently, we focus our discussion on p-nitrophenyl isothiocyanate in the following.

For a profound understanding of the changes in p-nitrophenyl isothiocyanate during reaction with the zinc complex, a clear assignment of the Raman bands of p-nitrophenyl isothiocyanate is necessary. As shown in Figure 3, the DFT-calculated Raman spectrum of p-nitrophenyl isothiocyanate fits well the corresponding
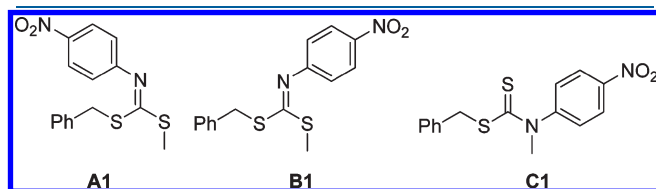
Figure 2. GC/MS results. Conceivable products of the quenching reaction with methyl iodide: **A1**, (Z)-benzylmethyl (4-nitrophenyl)carbonimidodithioate; **B1**, (E)-benzylmethyl (4-nitrophenyl)-carbonimidodithioate; **C1**, benzyl methyl(4-nitrophenyl)carbamodithioate.

Table 4. Free Gibbs Enthalpies Referring to Scheme 5 Relative to the Separated Reactants $[Zn(NH_3)_3SMe]^+$, R-Isothiocyanate, and Methyl Mercaptan at the B3LYP/6-311+G(d,p) Level of Theory

	R = Me		R = Me*[a]		R = Ph		R = Ph*		R = p-NO$_2$-Ph		R = p-NO$_2$-Ph*	
	ΔG	$\Delta\Delta G_a$[b]	ΔG	$\Delta\Delta G_a$	ΔG	$\Delta\Delta G_a$	ΔG	$\Delta\Delta G_a$	ΔG	$\Delta\Delta G_a$	ΔG	$\Delta\Delta G_a$
N6-AF	31		91		31		94		46		88	
N7-AF(ts)	109	78	186	95	116	85	201	107	132	86	189	101
N8-AF	5		59		19		71		36		71	
6-BS	43		96		32		95		51		78	
7-BS(ts)	91	48	156	60	95	63	153	58	103	52	128	50
8-BS	5		60		19		75		36		80	
U-10	−10		22		−8		−12		−6		−14	

[a] Columns with stars represent solvent calculations in DMSO. [b] Activation energy relative to the preceding intermediate.

experimentally determined Raman spectra of the DMSO solution. The normal mode assignment is shown in Table 6. Because the Raman band at 2111 cm^{-1} in the Raman spectrum of the DMSO solution is broad and weak,[23] we varied the solvent and obtained a well-pronounced Raman signal at 2099 cm^{-1} when using CH$_3$Cl instead of DMSO (cf. the Supporting Information). In contrast to the well-localized vibrations of the C≡N triple bond, vibrations of the C—S bond are always associated with the strong stretching vibrations of the nitro group calculated to result in intense Raman bands at 1302 and 1288 cm^{-1}.

Indeed, the wavenumber shift between the latter Raman bands corresponding to the nitro group is the only discrepancy between the experiment and theory. This is an artifact of the level of theory used. A further discussion can be found in the Supporting Information.

Table 5. Yields of the Zinc-Complex-Mediated Reaction of Isothiocyanates To Give Dithiocarbamates (%) at Room Temperature (Derived from the GC Spectra)

substituent	12Bn	i14Bn	14Bn	15Bn
Me	a	a	21	18
Ph	>1[b]	76	72	94
p-NO$_2$-Ph	72	88	81	87

[a] These reactions did not take place. [b] This reaction took place but gave poor product yield.

Furthermore, we analyzed the Raman spectra of the solid and dissolved zinc complex. Because no significant changes are found in the Raman spectra of the macrocyclic ligand during the reaction and the Raman signals of the complex are weak compared to the ones of p-nitrophenyl isothiocyanate, the Raman spectra of the complexes are not discussed in the present paper.

Focusing on the product formation, predominantly changes of the above-discussed Raman bands of p-nitrophenyl isothiocyanate, which are assigned to the cumulene system, are expected. Following our NRT calculation described in the previous section, the C—N bond in the isothiocyanate group loses the triple-bond character upon addition to the C—N and C—S bonds. Consequently, the CN vibrational mode is not suitable to unravel the reaction mechanism. Anyhow, in accordance to this prediction, the 2111 cm^{-1} mode disappears in the experimental Raman spectra within 1 or 2 s because of product formation (cf. Figure 4). Considering the modes involving C—S bond stretching, i.e., 1343 and 1258 cm^{-1} in the experimental Raman spectrum of p-nitrophenyl isothiocyanate, the DFT calculations predict a vanishing of the latter mode, while the Raman bands appear between 1200 and 1350 cm^{-1} in either mode of product formation. In contrast, the Raman signal referring to the vibration involving the nitrophenyl group and the C—S bond (1343/1302 cm^{-1} in the experimental/DFT-calculated Raman spectrum of p-nitrophenyl isothiocyanate) is shifted to 1316 cm^{-1} and gets strongly intensified because of product formation in the experimental Raman spectra of 15Bn, i14Bn, and 14Bn, as shown in Figure 4. Thus, the experimental Raman signal at
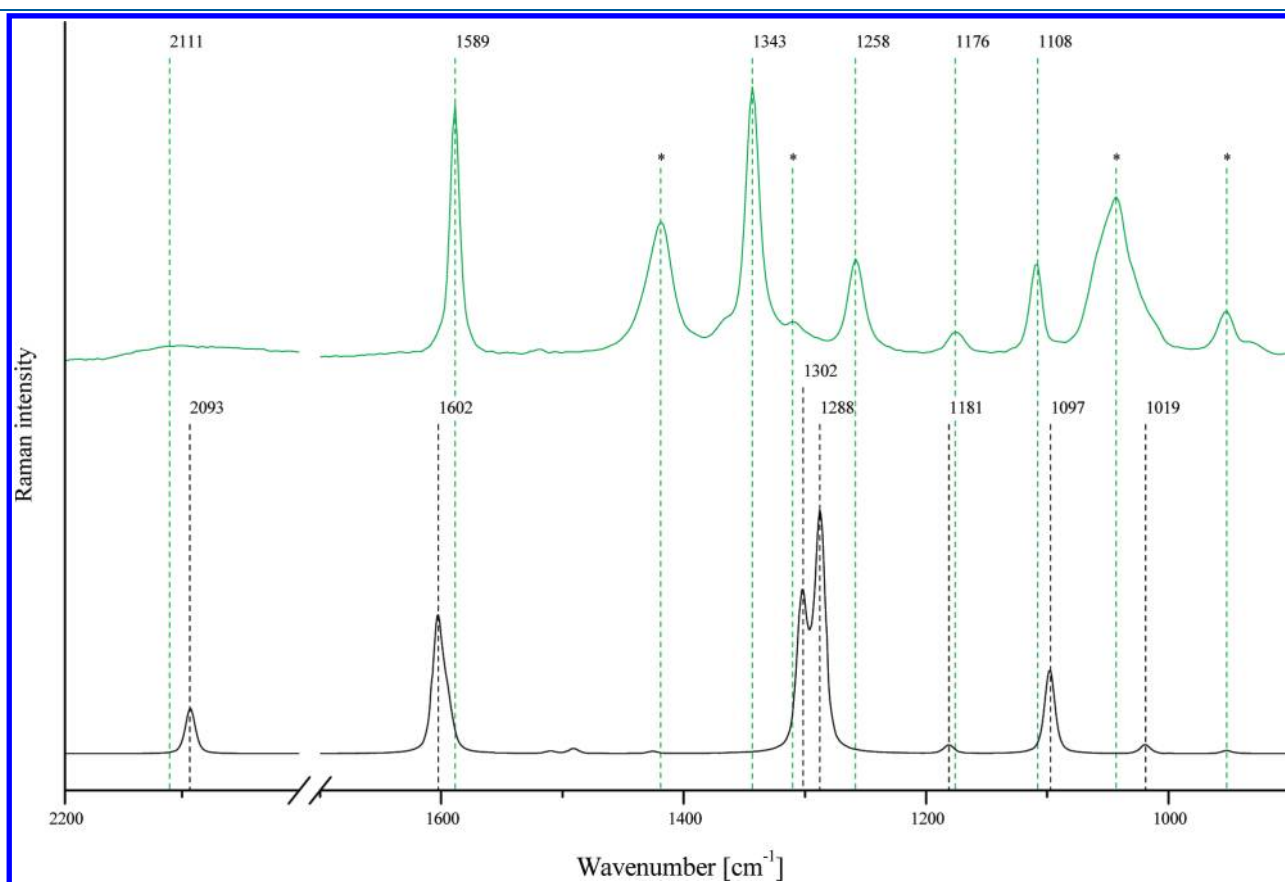

Figure 3. Green: Experimental Raman spectrum of p-nitrophenyl isothiocyanate dissolved in DMSO. DMSO Raman bands are marked by asterisks. Black: DFT-calculated Raman spectrum of p-nitrophenyl isothiocyanate.

Table 6. Assignment of the Vibrational Modes in the Raman Spectra of *p*-Nitrophenyl Isothiocyanate (Calculated and Experimentally Derived in DMSO and Chloroform)[a]

$\tilde{\nu}_{calc}$ [cm^{-1}]	$\tilde{\nu}_{DMSO}$ [cm^{-1}]	$\tilde{\nu}_{CHCl_3}$ [cm^{-1}]	description
2093	2111	2099	ν(CN)
1602	1589	1589	δ^{ip}(ph)
1302	1343	1335	ν[C—N(O$_2$)] + weak ν(CN + CS)
1288	1258	1266	ν[C—N(O$_2$)] + strong ν(CN + CS)
1181	1174	1174	δ^{ip}(ph)
1097	1108	1107	ν[C—N(O$_2$)] + δ^{ip}(ph)
1019	[b]	1013	δ^{ip}(ph)

[a] δ_{ip}: in-plane deformation vibrations. ν: stretching vibrations. [b] Peak is overlapped by a solvent band.
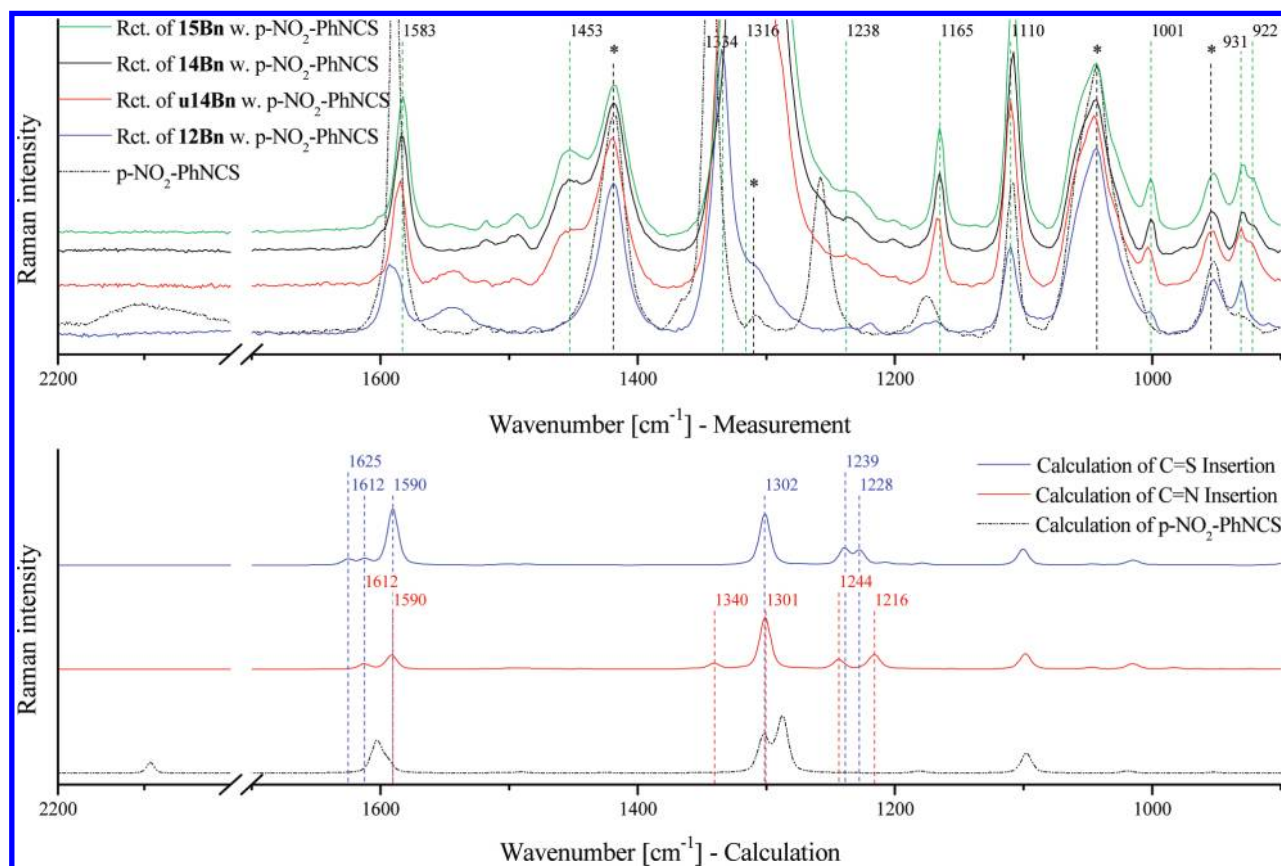
Figure 4. Top: Experimental product Raman spectra of the reaction of *p*-nitrophenyl isothiocyanate with complexes **15Bn**, **i14Bn**, **14Bn**, and **12Bn** dissolved in DMSO (solvent bands areindicated by asterisks). Bottom: DFT-calculated Raman spectra of the products emerging from the different reaction mechanisms (C—N or C—S insertion). The dotted graphs depict unreacted isothiocyanate.

1316 cm^{-1} is much more intense than the Raman signal at 1583 cm^{-1}, which corresponds to the calculated Raman spectra in the case of C—N insertion. Therefore, it seems reasonable that in the case of these complexes the preferred reaction mechanism is the insertion of the thiolate ligand into the C—N bond. This conclusion is further supported by the Raman band at 1453 cm^{-1}, which is predicted by the calculated Raman spectra but with a very low intensity. The latter band is assigned to a mode involving phenyl—N bond stretchings and vibrations of the azamacrocycle ligands. Apparently, the level of theory has problems handling the intensities of the macrocyclic ligand bands properly.

12Bn gives a different spectrum because the peak around 1600 cm^{-1} is broader and slightly shifted to higher wavenumber values. This change can be explained by a C=N double bond

emerging upon product formation via insertion into the C—S bond (cf. the Zinc-Complex-Mediated Reactions section). Furthermore, the DFT calculations predict almost equally intense Raman bands at 1302 and 1590 cm^{-1} in the case of C—S insertion, as shown in Figure 4. This is supported by the experimental Raman spectrum of **12Bn** because the Raman intensity of the mode involving the nitro group (1334 cm^{-1}) is significantly reduced in comparison to the previously discussed complexes (**15Bn**, **i14Bn**, and **14Bn**). Thus, in the case of **12Bn**, the Raman intensity of the mode at 1334 cm^{-1} approaches the order of intensity of the Raman band at 1595 cm^{-1}.

These results indicate a preference of insertion into the C=N double bond in most cases. This correlates well with the prediction of the higher electron density in this bond. However,

3230

dx.doi.org/10.1021/ic101464j |*Inorg. Chem.* 2011, 50, 3223–3233

the influence of the azamacrocyclic ligand becomes significant in the example of **12Bn** because in this case the alternative insertion into the C—S bond seems to be preferred. Further vibrational assignments of the Raman bands calculated for the different reaction mechanisms are given in the Supporting Information.

■ CONCLUSION

In this work, we examined the translation of an enzymatic mode of action principle to a synthetic scenario. Therefore, exhaustive DFT calculations were performed to predict possible reaction paths. Subsequently, a variety of potential catalysts was synthesized to identify the conditions to follow the desired reaction paths and to obtain the aspired products.

Because of the unsymmetrical cumulated bond system in isothiocyanates, the number of conceivable reaction paths expands into a huge manifold of similar alternatives, which is quite difficult to handle compared to the natural zinc-complex-mediated standard reaction of the initial $CA/CO_2/H_2O$ system. Nevertheless, from these investigations, we conclude that the natural paragon, the activation and hydration of CO_2 and COS by specific zinc enzymes (CAs), can be applied to a much wider number of cumulenic substrates and zinc complex variants than previously assumed because the zinc thiolate complex definitely inserts into the cumulene system of isothiocyanate at room temperature. We demonstrated that these $[L_nZn-SR]^+$ complexes are able to induce reaction mechanisms similar to those of their oxygen analogues, the *nucleophilic* $[L_nZn-OH]^+$ *cation complexes*, i.e., the activation of a variety of isothiocyanates to open further addition reaction paths. Unfortunately, the activation of isothiocyanates by $[L_nZn-SR]^+$ complexes is not sufficiently reactive to allow the addition of the corresponding mercaptans, which would initiate a catalytic cycle analogously to the natural "$CA/CO_2/H_2O$" mode of action. Further, at this point the predictions of the calculations are not reliable throughout because they result in a surmountable transition state. The selectivity problem (C═N vs C═S) can also not be solved completely by DFT calculations alone, but this is due to relatively small energy differences. In contrast, our Raman spectroscopic investigations verify that the C═N bond of the aryl isothiocyanate structures is the preferred moiety to be attacked by the cationic but nucleophilic $[L_nZn-SR]^+$ complexes. This is in good agreement with the more stable intermediate **N5-A**, which is in equilibrium with the C═S insertion product **5-A**. The activation barrier of the most probable pathway, i.e., **2(ts)** (cf. Scheme 3), is reduced by 60—30 kJ/mol compared to the nonactivated (or standard) reaction path (cf. Figure 2) and depends on the isothiocyanate used. Another unfavored alternative via **N2(ts)** is conceivable but can lead to the same product **U-10** (cf. Schemes 4 and 5). Additionally, we could reproduce the reactivity of the zinc thiolate complexes depending on the ring size of their ligands found in the reaction with CS_2.

These possibilities are, of course, structurally and conceptually far beyond the natural mode of action of the CAs as catalysts, which stand out because of their efficiency in transforming the substrates CO_2 and COS. However, the aim of this work was not to reinvestigate the reaction principles of CAs but rather to understand and finally to translate the basic reaction sequences in order to estimate whether they might be applicable in synthesis or not. Therefore, we combined theoretical studies (DFT and ab initio calculations, if possible under inclusion of solvent effects) with experimental investigations (GC/MS and Raman spectroscopy).

This combination serves as a powerful tool to develop novel and efficient syntheses modeled on nature.

■ EXPERIMENTAL SECTION

Materials and Methods. All reagents used were of analytical purity. GC/MS data were recorded on a Shimadzu GC-2010 mass spectrometer (GCMS-QP2010S), Ultra Alloy+ −5 capillary column, 30 m × 0.25 mm i.d., 0.25 μm film (Frontier Laboratories), and a standard program at 2 min at 40 °C, followed by a temperature increase of 16 °C/min, and held at 250 °C for 5 min.

Raman spectra of solid samples were recorded with a Jobin-Yvon Labram HR spectrometer, equipped with an Olympus BX41 inverse microscope. The 830 nm output from a diode laser was used as the Raman excitation source, and the scattered light was detected with a CCD detector. A grating with 300 grooves/mm was applied, leading to a spectral resolution of roughly 1 cm^{-1}. The measurements were carried out in dry DMSO at room temperature. The Raman spectra of unreacted isothiocyanates were also measured in dry $CHCl_3$.

Preparation of Azamacrocycles. The azamacrocycles $[12]aneN_4$, $[14]aneN_4$, i-$[14]aneN_4$, and $[15]aneN_4$ were synthesized using the usual Richman—Atkins method.[24] Some changes in the procedure developed in our work group were applied to this synthesis.[16]

Preparation of the Zinc Thiolate Complexes. In general, the thiolate complexes were synthesized as described previously.[16] However, some changes were made to achieve a better yield in the case of **12Bn** and **15Bn**.

The yield of $[Zn([15]aneN_4)(SBn)]ClO_4$ (**15Bn**) could be increased from 35% to 76% by using 8 mmol of the ligand, 40 mL of a 0.2 M solution of $Zn(ClO_4)_2 \cdot 6H_2O$ in methanol, and 8 mL of a 0.5 M solution of KOH in methanol. The solution was kept in the freezer at −40 °C to allow it precipitate properly. In the case of $[Zn([12]aneN_4)-(SBn)]ClO_4$ (**12Bn**), it was possible to increase the yield from 35% to 73% by using 8 mmol of the ligand, 80 mL of a 0.1 M solution of $Zn(ClO_4)_2 \cdot 6H_2O$ in methanol, and 8 mL of a 0.5 M solution of KOH in methanol.

Reaction of the Zinc Thiolate Complexes with Isothiocyanates To Give Dithiocarbamates. All reactions were performed in dry DMSO under standard conditions and at room temperature. A total of 0.5 mL of a 0.1 M solution of isothiocyanate was slowly added into 0.5 mL of a 0.1 M solution of the thiolate complex. After 10 min of stirring, an equimolar amount of methyl iodide was added, and the mixture was filtered and immediately examined via GC/MS. All reaction solutions have a pale-yellow color; in the case of *p*-nitrophenyl isothiocyanate, the color is strong yellow and turns into a deep red immediately after the addition of isothiocyanate to the zinc thiolate complex. After the addition of methyl iodide, the color slowly returns to yellow.

Regarding the Raman measurement, the same procedure, except the addition of methyl iodide, was used.

Computational Methods. All optimizations and frequency calculations reported in this Article were performed using the *Gaussian03* program package.[25] Atomic charges and hyperconjugative interaction energies were obtained using version 5.1 of the natural bond orbital (NBO) analysis of Weinhold et al. in *Gaussian03*, which is not included in Gaussian by default.[20,26] Default convergence criteria were used for all calculations. All energies reported are Gibbs free energies (ΔG values relative to the separated reactants) and thus contain zero-point, thermal, and entropy effects at 298 K and 1 atm pressure.

The hybrid density functional B3LYP[27] with the 6-311+G(d,p) basis set[28] was used throughout for the zinc-complex-mediated reaction. Previous investigations have demonstrated reliable results on this level of theory for systems like $[Zn(NH_3)_3OH]^+$.[8−10] The standard reaction was calculated at the MP2 level[29] using the aug-cc-pVDZ[30] basis due to

3231

dx.doi.org/10.1021/ic101464j |*Inorg. Chem.* 2011, 50, 3223–3233

the smaller system. Full geometry optimizations, i.e., without constraints, as well as frequency calculations on the stationary points thus obtained were performed for all species on the hypersurface in the gas phase as well as in the presence of a dielectric field as described by the C-PCM model for selected structures.[31] In this model, the species of interest are embedded in a cavity of molecular shape surrounded by a polarizable continuum whose field modifies the energy and physical properties of the solute. The solvent reaction field is described by polarization charges distributed on the cavity surface. This procedure is known to reproduce experimental solvation energies quite well. We chose the solvent DMSO used in the experimental investigations. Because of the better PCM model implemented in *Gaussian09*,[32] the solvent corrections have been calculated using this newer version of that program. The gas-phase reactions have been calculated with *Gaussian03* only for historical reasons and are fully comparable to the *Gaussian09* PCM calculations.

For calculation of the Raman spectra, we used BP86/TZVP because this combination turned out to give accurate molecular structures, frequencies, and Raman intensities for medium-sized molecules.[33] Furthermore, there is no need to scale the obtained wavenumbers of the vibrational normal modes to adjust them to experimental values.[22]

■ ASSOCIATED CONTENT

ⓢ Supporting Information. Cartesian coordinates of all stationary points as well as relative free energies not listed in the paper, all total energies, and a detailed discussion of the Raman spectra. This material is available free of charge via the Internet at http://pubs.acs.org.

■ AUTHOR INFORMATION

Corresponding Author

*E-mail: ernst.anders@uni-jena.de.

■ ACKNOWLEDGMENT

■ REFERENCES

(1) (a) Bertini, I.; Luchinat, C. *Acc. Chem. Res.* **1983**, *16*, 272. (b) Christianson, D. W.; Fierke, C. A. *Acc. Chem. Res.* **1996**, *29*, 331. (c) Coleman, J. E. *J. Biol. Chem.* **1967**, *242*, 5212. (d) Lindskog, S. *Pharmacol. Ther.* **1997**, *74*, 1. (e) Lindskog, S.; Liljas, A. *Curr. Opin. Struct. Biol.* **1993**, *3*, 915.(f) Silverman, D. N. In *Enzyme Kinetics and Mechanism Part D: Developments in Enzyme Dynamics*; Purich, D. L., Ed.; Academic Press: New York, 1995; Vol. 249, p 479. (g) Silverman, D. N.; Lindskog, S. *Acc. Chem. Res.* **1988**, *21*, 30.

(2) Khalifah, R. G. *J. Biol. Chem.* **1971**, *246*, 2561.

(3) Pocker, Y.; Stone, J. T. *J. Am. Chem. Soc.* **1965**, *87*, 5497.

(4) (a) Sly, W. S.; Hu, P. Y. *Annu. Rev. Biochem.* **1995**, *64*, 375. (b) Supuran, C. T.; Scozzafava, A.; Casini, A. *Med. Res. Rev.* **2003**, *23*, 146.

(5) Hewett-Emmett, D.; Tashian, R. E. *Mol. Phylogenet. Evol.* **1996**, *5*, 50.

(6) Jahn, B. O.; Eger, W. A.; Anders, E. In *Biomimetics Learning from Nature*; Mukherjee, A., Ed.; INTECH: Vienna, Austria, 2010; p 167.

(7) (a) Bottoni, A.; Lanza, C. Z.; Miscione, G. P.; Spinelli, D. *J. Am. Chem. Soc.* **2004**, *126*, 1542. (b) Bräuer, M.; Anders, E.; Sinnecker, S.; Koch, W.; Rombach, M.; Brombacher, H.; Vahrenkamp, H. *Chem. Commun.* **2000**, *1*, 647. (c) Bräuer, M.; Perez-Lustres, J. L.; Weston, J.; Anders, E. *Inorg. Chem.* **2002**, *41*, 1454. (d) Mauksch, M.; Bräuer, M.;

Weston, J.; Anders, E. *ChemBioChem* **2001**, *2*, 190. (e) Merz, K. M.; Banci, L. *J. Phys. Chem.* **1996**, *100*, 17414. (f) Miscione, G.; Stenta, M.; Spinelli, D.; Anders, E.; Bottoni, A. *Theor. Chem. Acc.* **2007**, *118*, 193.

(8) (a) Schenk, S.; Kesselmeier, J.; Anders, E. *Chem.—Eur. J.* **2004**, *10*, 3091. (b) Notni, J.; Schenk, S.; Protoschill-Krebs, G.; Kesselmeier, J.; Anders, E. *ChemBioChem* **2007**, *8*, 530.

(9) (a) Jahn, B. O.; Eger, W. A.; Anders, E. *J. Org. Chem.* **2008**, *73*, 8265. (b) Jahn, B. O.; Eger, W. A.; Anders, E. *Z. Naturforsch.* **2010**, *65b*, 425.

(10) Eger, W. A.; Jahn, B. O.; Anders, E. *J. Mol. Model.* **2009**, *15*, 443.

(11) Notni, J.; Schenk, S.; Roth, A.; Plass, W.; Görls, H.; Uhlemann, U.; Walter, A.; Schmitt, M.; Popp, J.; Chatzipapadopoulos, S.; Emmler, T.; Breitzke, H.; Leppert, J.; Buntkowsky, G.; Kempe, K.; Anders, E. *Eur. J. Inorg. Chem.* **2006**, *14*, 2783.

(12) (a) von Wrochem, F.; Gao, D.; Scholz, F.; Nothofer, H.-G.; Nelles, G.; Wessels, J. M. *Nat. Nanotechnol.* **2010**, *5*, 618. (b) Vickers, M. S.; Cookson, J.; Beer, P. D.; Bishop, P. T.; Thiebaut, B. *J. Mater. Chem.* **2006**, *16*, 209. (c) Zhao, Y.; Pérez-Segarra, W.; Shi, Q.; Wei, A. *J. Am. Chem. Soc.* **2005**, *127*, 7328. (d) Schulz, P.; Zangmeister, C. D.; Zhao, Y.-L.; Frail, P. R.; Saudari, S. R.; Gonzalez, C. A.; Kagan, C. R.; Wuttig, M.; Zee, R. D. v. *J. Phys. Chem. C* **2010**, *114*, 20843.

(13) (a) Halls, D. J. *Microchim. Acta* **1969**, *57*, 62. (b) Malik, A. K.; Faubel, W. *Pestic. Sci.* **1999**, *55*, 965.

(14) Schröder, D.; Schwarz, H.; Schenk, S.; Anders, E. *Angew. Chem.* **2003**, *115*, 5241.

(15) (a) Kimura, E.; Shiota, T.; Koike, T.; Shiro, M.; Kodama, M. *J. Am. Chem. Soc.* **1990**, *112*, 5805. (b) Zhang, X.; van Eldik, R. *Inorg. Chem.* **1995**, *34*, 5606. (c) Zhang, X.; van Eldik, R.; Koike, T.; Kimura, E. *Inorg. Chem.* **1993**, *32*, 5749.

(16) Notni, J.; Görls, H.; Anders, E. *Eur. J. Inorg. Chem.* **2006**, *7*, 1444.

(17) Notni, J.; Günther, W.; Anders, E. *Eur. J. Inorg. Chem.* **2007**, *7*, 985.

(18) (a) Liang, J. Y.; Lipscomb, W. N. *Biochemistry* **1987**, *26*, 5293. (b) Sola, M.; Lledos, A.; Duran, M.; Bertran, J. *J. Am. Chem. Soc.* **1992**, *114*, 869. (c) Tautermann, C. S.; Loferer, M. J.; Voegele, A. F.; Liedl, K. R. *J. Phys. Chem. B* **2003**, *107*, 12013.

(19) Lindskog, S.; Engberg, P.; Forsman, C.; Ibrahim, A. S.; Jonsson, H. B.; Simonsson, I.; Tibell, L. *Ann. N.Y. Acad. Sci.* **1987**, *429*, 61.

(20) (a) Glendening, E. D.; Badenhoop, J. K.; Reed, A. E.; Carpenter, J. E.; Bohmann, J. A.; Morales, C. M.; Weinhold, F. *NBO*; University of Wisconsin: Madison, WI, 2001. (b) Reed, A. E.; Curtiss, L. A.; Weinhold, F. *Chem. Rev. (Washington, DC, U.S.)* **1988**, *88*, 899.

(21) (a) Presselt, M.; Schnedermann, C.; Schmitt, M.; Popp, J. *J. Phys. Chem. A* **2009**, *113*, 3210. (b) Presselt, M.; Dietzek, B.; Schmitt, M.; Rau, S.; Winter, A.; Jäger, M.; Schubert, U. S.; Popp, J. *J. Phys. Chem. A* **2010**, *114*, 13163.

(22) (a) Presselt, M.; Dietzek, B.; Schmitt, M.; Popp, J.; Winter, A.; Chiper, M.; Friebe, C.; Schubert, U. S. *J. Phys. Chem. C* **2008**, *112*, 18651. (b) Winter, A.; Friebe, C.; Chiper, M.; Schubert, U. S.; Presselt, M.; Dietzek, B.; Schmitt, M.; Popp, J. *ChemPhysChem* **2009**, *10*, 787.

(23) (a) Joo, S.-W. *Surf. Interface Anal.* **2006**, *38*, 173. (b) Stephenson, C. V.; Coburn, W. C.; Wilcox, W. S. *Spectrochim. Acta* **1961**, *17*, 933.

(24) Richman, J. E.; Atkins, T. J. *J. Am. Chem. Soc.* **1974**, *96*, 2268.

(25) Frisch, M. J.; Trucks, G. W.; Schlegel, H. B.; Scuseria, G. E.; Robb, M. A.; Cheeseman, J. R.; Montgomery, J. J. A.; Vreven, T.; Kudin, K. N.; Burant, J. C.; Millam, J. M.; Iyengar, S. S.; Tomasi, J.; Barone, V.; Mennucci, B.; Cossi, M.; Scalmani, G.; Rega, N.; Petersson, G. A.; Nakatsuji, H.; Hada, M.; Ehara, M.; Toyota, K.; Fukuda, R.; Hasegawa, J.; Ishida, M.; Nakajima, T.; Honda, Y.; Kitao, O.; Nakai, H.; Klene, M.; Li, X.; Knox, J. E.; Hratchian, H. P.; Cross, J. B.; Bakken, V.; Adamo, C.; Jaramillo, J.; Gomperts, R.; Stratmann, R. E.; Yazyev, O.; Austin, A. J.; Cammi, R.; Pomelli, C.; Ochterski, J. W.; Ayala, P. Y.; Morokuma, K.; Voth, G. A.; Salvador, P.; Dannenberg, J. J.; Zakrzewski, V. G.; Dapprich, S.; Daniels, A. D.; Strain, M. C.; Farkas, O.; Malick, D. K.; Rabuck, A. D.; Raghavachari, K.; Foresman, J. B.; Ortiz, J. V.; Cui, Q.; Baboul, A. G.; Clifford, S.; Cioslowski, J.; Stefanov, B. B.; Liu, G.; Liashenko, A.; Piskorz, P.; Komaromi, I.; Martin, R. L.; Fox, D. J.; Keith, T.; Al-Laham,

M. A.; Peng, C. Y.; Nanayakkara, A.; Challacombe, M.; Gill, P. M. W.; Johnson, B.; Chen, W.; Wong, M. W.; Gonzalez, C.; Pople, J. A. *Gaussian03*, revision C.01; Gaussian Inc.: Wallingford, CT, 2004.

(26) (a) Reed, A. E.; Weinhold, F. *J. Chem. Phys.* **1983**, *78*, 4066. (b) Reed, A. E.; Weinstock, R. B.; Weinhold, F. *J. Chem. Phys.* **1985**, *83*, 735.

(27) (a) Becke, A. D. *J. Chem. Phys.* **1993**, *98*, 5648. (b) Lee, C.; Yang, W.; Parr, R. G. *Phys. Rev. B* **1988**, *37*, 785.

(28) (a) Krishnan, R.; Binkley, J. S.; Seeger, R.; Pople, J. A. *J. Chem. Phys.* **1980**, *72*, 650. (b) McLean, A. D.; Chandler, G. S. *J. Chem. Phys.* **1980**, *72*, 5639.

(29) (a) Frisch, M. J.; Head-Gordon, M.; Pople, J. A. *Chem. Phys. Lett.* **1990**, *166*, 275. (b) Head-Gordon, M.; Pople, J. A.; Frisch, M. J. *Chem. Phys. Lett.* **1988**, *153*, 503.

(30) (a) Kendall, R. A.; Dunning, J. T. H.; Harrison, R. J. *J. Chem. Phys.* **1992**, *96*, 6796. (b) Woon, D. E.; Dunning, J. T. H. *J. Chem. Phys.* **1993**, *98*, 1358.

(31) (a) Barone, V.; Cossi, M. *J. Phys. Chem. A* **1998**, *102*, 1995. (b) Cossi, M.; Rega, N.; Scalmani, G.; Barone, V. *J. Comput. Chem.* **2003**, *24*, 669. (c) Klamt, A.; Schüürmann, G. *J. Chem. Soc., Perkin Trans. 2* **1993**, 799.

(32) Frisch, M. J.; Trucks, G. W.; Schlegel, H. B.; Scuseria, G. E.; Robb, M. A.; Cheeseman, J. R.; Scalmani, G.; Barone, V.; Mennucci, B.; Petersson, G. A.; Nakatsuji, H.; Caricato, M.; Li, X.; Hratchian, H. P.; Izmaylov, A. F.; Bloino, J.; Zheng, G.; Sonnenberg, J. L.; Hada, M.; Ehara, M.; Toyota, K.; Fukuda, R.; Hasegawa, J.; Ishida, M.; Nakajima, T.; Honda, Y.; Kitao, O.; Nakai, H.; Vreven, T.; Montgomery, J. A., Jr.; Peralta, J. E.; Ogliaro, F.; Bearpark, M.; Heyd, J. J.; Brothers, E.; Kudin, K. N.; Staroverov, V. N.; Kobayashi, R.; Normand, J.; Raghavachari, K.; Rendell, A.; Burant, J. C.; Iyengar, S. S.; Tomasi, J.; Cossi, M.; Rega, N.; Millam, N. J.; Klene, M.; Knox, J. E.; Cross, J. B.; Bakken, V.; Adamo, C.; Jaramillo, J.; Gomperts, R.; Stratmann, R. E.; Yazyev, O.; Austin, A. J.; Cammi, R.; Pomelli, C.; Ochterski, J. W.; Martin, R. L.; Morokuma, K.; Zakrzewski, V. G.; Voth, G. A.; Salvador, P.; Dannenberg, J. J.; Dapprich, S.; Daniels, A. D.; Farkas, Ö.; Foresman, J. B.; Ortiz, J. V.; Cioslowski, J.; Fox, D. J. *Gaussian09*, revision A.01; Gaussian Inc.: Wallingford, CT, 2009.

(33) (a) Neugebauer, J.; Hess, B. A. *J. Chem. Phys.* **2003**, *118*, 7215. (b) Reiher, M.; Brehm, G.; Schneider, S. *J. Phys. Chem. A* **2004**, *108*, 734. (c) Reiher, M.; Neugebauer, J.; Hess, B. A. *Z. Physik. Chem.* **2000**, *118*, 7215.